VOL. 15, NO. 22, NOVEMBER 2020 ISSN 1819-6608
ARPN Journal of Engineering and Applied Sciences

www.arpnjournals.com

PRESSURE AND PRESSURE DERIVATIVE ANALYSIS WITH INTER-RESERVOIR CROSS FLOW RATE BETWEEN ADJACENT RESERVOIR LAYERS

Freddy H. Escobar[1], Daniel Suescún-Díaz[2] and José Miguel Galindo[1]
[1]Universidad Sur Colombiana/CENIGAA, Avenida Pastrana - Cra, Neiva, Huila, Colombia
[2]Departamento de Ciencias Naturales, Avenida Pastrana, Universidad Sur colombiana, Neiva, Huila, Colombia
E-Mail: fescobar@usco.edu.co

ABSTRACT

An appropriate characterization of a two-layer interconnected system is of vital importance for reservoir appraisal and administration. In this work, the *TDS* Technique is used for the interpretation of transient pressure test of a two-layer system separated by a low-permeable stratum so its specific permeability and the permeability of the adjacent layer can be estimated. The new developed expressions were applied to one synthetic example when the flow capacity of layer 1 is higher than layer 2. Another simulated example was devoted to the inverted flow capacity case. The average absolute deviation errors for specific permeability is lower than 1.2 % and for layer 2 permeability is lower than 0.1 % demonstrating the accuracy and convenience of the methodology.

Keywords: cross flow, composite reservoirs, radial flow, horizontal permeability, second pressure derivative.

1. INTRODUCTION

Many reservoir systems have more than one layer with hydraulic communication among them. Rahman, Bin Akresh, and Al-Thawad (2015) presented pressure and pressure derivative behavior for a two-layer system communicated behind the casing due to poor cementing jobs. During transient tests, the fluid in the adjacent layer may still migrate and contribute to the tested layer, if the integrity of cement is deteriorated or flow paths exist between them, leading an over-estimation of the productive capability of the tested reservoir layer. The mathematical model for such case was developed by Rahman (2014). Later, Escobar, Palomino and Ghisays-Ruiz (2019) extended the *TDS* Technique, Tiab (1995), for interpretation of pressure tests with interconnection between two adjacent layers through leaks behind the casing using the model proposed by Rahman (2014). Escobar, Palomino and Ghisays-Ruiz (2019) identified a new flow regime, called radi-linear, which results from the simultaneous action of the radial horizontal flow regime with the vertical linear flow along the cement shaft.

Because flow must be diagnosed to accurately characterize a tested layer, a new analytical method is proposed by Rahman and Nooruddin (2016) to estimate the effects of cross flow on the transient pressure behavior by quantifying the hydraulic conductivity or specific permeability, F_{cb}, between two layers separated by a low-permeable stratum. The value of F_c is used to determinate the contribution from an adjacent layer to the production of the tested layer through the wellbore, corresponding to a pressure at a given time. Detecting cross flow and understanding the degree of the communication is essential from a production and reservoir engineering perspective in accordance with Jalali *et al* (2016). It allows capturing the real performance of the reservoir in order to improve its management and development as presented by Al-Wehaibi, Anisur and Issaka (2016).

Rahman and Nooruddin (2016) presented an analytical solution considering the effect of the hydraulic conductivity when cross flow from an adjacent layer takes place between a reservoir systems composed by two adjacent layers separated by a low permeability stratum. Later, the pressure derivative behaviors were studied by Nooruddin and Rahman (2017). They demonstrated that once radial flow is affected by the low-permeable, the pressure derivative adopts an inverted S-shape during the response of the low-permeable stratum and, then, a second plateau is developed because of the other adjacent layer. In this work, the model of Rahman and Nooruddin (2016) was employed to extend the application of the *TDS* Technique, Tiab (1995) to estimate the specific permeability of the interbedded low-permeable stratum and the permeability of the second reservoir layer, as well. The obtained results were successfully applied to synthetic examples. Further, later and extensive applications of the *TDS* Technique can be found in the works of Escobar, Hernandez and Jongkittinarukorn (2018) and the books by Escobar (2018, 2109).

2. MATHEMATICAL TREATMENT

The mathematical model to account for the transient pressure behavior of a layer separated from another one by a low-permeable stratum with a hydraulic conductivity, F_{cb}, and the crossflow rate throughout the semi-permeable stratum, respectively, were presented by Rahman and Nooruddin (2016):

$$\overline{P}_{wf}=\frac{P_0}{l}-\frac{qB\left\{K_0\left(\sigma_1 r_{wa1}\right)-\frac{\beta_1}{\beta_2}K_0\left(\sigma_2 r_{wa1}\right)\right\}}{l\left[24Cl\left\{K_0\left(\sigma_1 r_{wa1}\right)-\frac{\beta_1}{\beta_2}K_0\left(\sigma_2 r_{wa1}\right)\right\}+\alpha_1\left\{\sigma_1 K_1\left(\sigma_1 r_{w1}\right)-\frac{\beta_1}{\beta_2}\sigma_2 K_1\left(\sigma_2 r_{w1}\right)\right\}\right]} \quad (1)$$

$$\overline{q_2 B_o}=\frac{qBX\left[\frac{(1-\beta_1)}{\sigma_1^2}-\frac{\beta_1(1-\beta_2)}{\beta_2\sigma_2^2}\right]}{141.2\mu l\left[24Cl\left\{K_0\left(\sigma_1 r_{wa1}\right)-\frac{\beta_1}{\beta_2}K_0\left(\sigma_2 r_{wa1}\right)\right\}+\alpha_1\left\{\sigma_1 K_1\left(\sigma_1 r_{w1}\right)-\frac{\beta_1}{\beta_2}\sigma_2 K_1\left(\sigma_2 r_{w1}\right)\right\}\right]} \quad (2)$$

Where the specific permeability of the semi-permeable barrier between the two layers and the maximum specific permeability are given by Nooruddin and Rahman (2017) are, respectively given by:

$$F_{cb} = \frac{2k_{v0}k_{v1}k_{v2}}{2h_0k_{v1}k_{v2} + h_1k_{v0}k_{v2} + h_2k_{v0}k_{v1}} \quad (3)$$

$$F_{cb}\,\max = \frac{2}{h_1/k_{v1} + h_2/k_{v2}} \quad (4)$$

Other parameters in Equations (1) and (2) are given in Appendix A.

The dimensionless quantities are defined by:

$$P_D = \frac{kh\Delta P}{141.2qB\mu} \quad (5)$$

$$t_D * P_D{}' = \frac{kh(t*\Delta P')}{141.2qB\mu} \quad (6)$$

$$t_D^2 * P_D{}'' = \frac{kh(t^2*\Delta P'')}{141.2qB\mu} \quad (7)$$

$$t_D = \frac{0.0002637kt}{\phi\mu c_t r_w^2} \quad (8)$$

The effect of the specific permeability on the pressure and pressure derivative behavior -obtained from Equation (1) - is given in Figure-1. Notice that the smaller the F_{cb} value the later the response of the second layer. At middle time, when radial flow in layer 1 dominates the transient behavior the dimensionless pressure derivative shows the usual behavior - a plateau - with a value of one half. It is followed by the effect of the low-permeable interlayer stratum forming an inverted "s-shape" behavior. After that, a second plateau responding for radial flow in layer 2 is developed. The system is assumed to possess infinite transient behavior. The value of the pressure derivative depends upon the flow capacity ratio, κ, defined as:

$$\kappa = \frac{k_2}{k_1}\frac{h_2}{h_1} \quad (9)$$

Figure-1 presents the pressure derivative behavior for five different values of the specific permeability of the semi-permeable barrier, F_{cb}. A unique behavior for the five systems is needed to determine the characteristic points which are employed for the development of the interpretation equations proper of the *TDS* Technique. The analysis for this achievement is given by Escobar, Bonilla and Hernández (2018). Notice in Figure-1 that the dimensionless time at which the deviation from the pressure derivative plateau increases as the specific permeability of the semi-permeable barrier decreases; then, for behavior unification purposes, the dimensionless time must be multiplied by the specific permeability of the semi-permeable barrier to the power n, where n is an unknown parameter that affects the unified behavior. To find the value of n an arbitrary point is chosen during the time between the two plateaus seen on the pressure derivative curve which is the matching zone of interest on the curve when F_{cb}= 1. The arbitrary chosen reference point was the inflection point. An analogous point is taken from another curve with F_{cb} different than 1. This procedure led to find an n value of one.

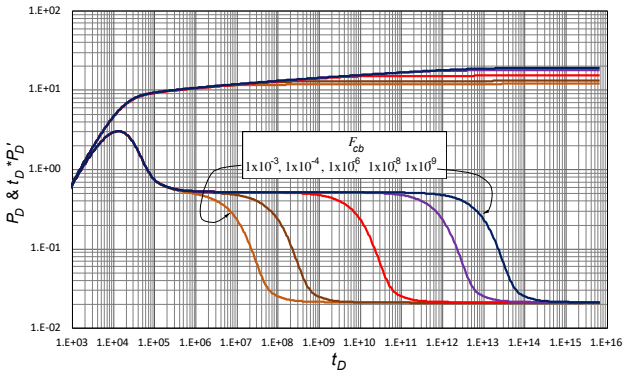

Figure-1. Dimensionless pressure and pressure derivative versus dimensionless time behavior for several F_{cb} values.

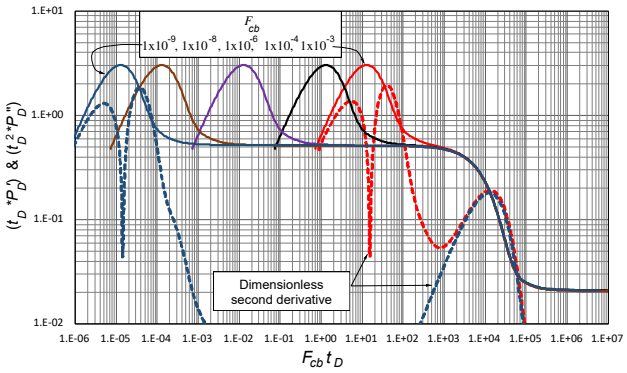

Figure-2. Dimensionless pressure, pressure derivative and some dimensionless second pressure derivative versus dimensionless time behavior for several F_{cb} values.

Figure-2 shows that the dimensionless time multiplied by F_{cb} provides unified curves of pressure, pressure derivative and second pressure derivative for a fixed value of κ. The effect of κ for a F_{cb} of 1x10^{-5} is given in Figure-3. Notice that as κ decreases so does the value of the maximum second pressure derivative and the minimum value of the pressure derivative increases. These above observations led to establish a relationship between the flow capacity ratio and ratios of pressure derivatives during the radial flow regimes of layers 1 and 2 as observed in Figure-4. From such plot results:

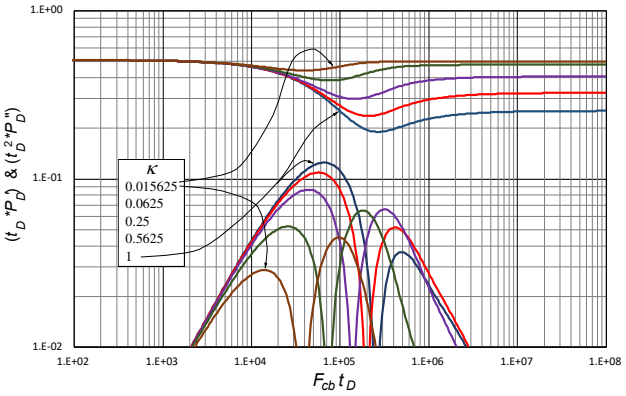

Figure-3. Dimensionless pressure derivative and dimensionless second pressure derivative versus dimensionless time behavior for F_{cb}= 1x10^{-5}.

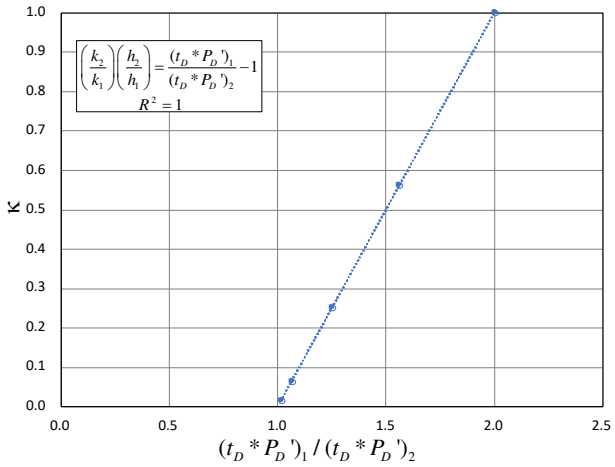

Figure-4. Relationship between κ and the pressure derivative plateau ratios.

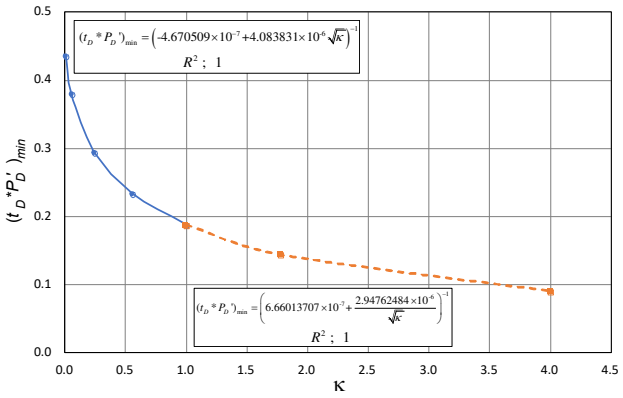

Figure-5. Relationship between κ and the minimum dimensionless pressure derivative during the effect of F_{cb}

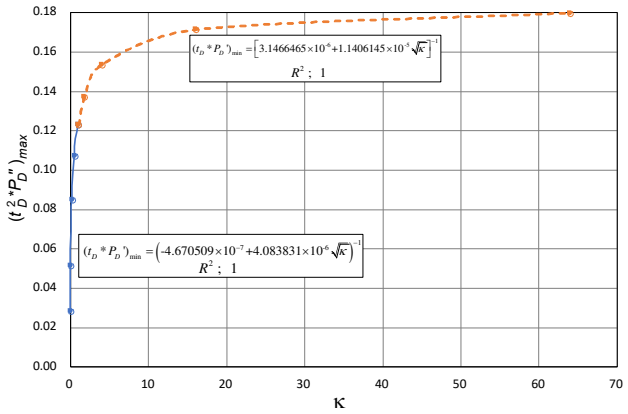

Figure-6. Relationship between κ and the maximum dimensionless second pressure derivative during the effect of F_{cb}.

$$\left(\frac{k_2}{k_1}\right)\left(\frac{h_2}{h_1}\right)=\frac{(t_D*P_D')_1}{(t_D*P_D')_2}-1 \tag{10}$$

After replacing Equations (6) and (9) into Equation (10) will result:

$$k_2=\left[\frac{(t*\Delta P')_1}{(t*\Delta P')_2}-1\right]\frac{k_1h_1}{h_2} \tag{11}$$

According to Tiab (1995) the permeability of layer 1 is estimated from:

$$k_1=\frac{70.6q\mu B}{h(t*\Delta P')_r} \tag{12}$$

Observations from Figures-5 and -6 lead to obtain a correcting value of both the minimum dimensionless pressure derivative and the second maximum dimensionless pressure derivative depending on the capacity ratios. This is performed by adjusting the relationship between either minimum pressure derivative or maximum pressure derivative against κ. That relationships are used to find a correction factor to move the minimum pressure derivative or maximum second pressure derivative to κof1.

Case 1: $k_1h_1 \geq k_2h_2$

The correction factor for effect of capacity ratio is given by:

$$\kappa_{CF}=\left(0.184439+\frac{0.81628396}{\sqrt{\kappa}}\right)^{-1} \tag{13}$$

And the governing expression for the minimum pressure derivative is:

$$F_{cb}(t_D)_{\min} = 277460.0873/\kappa_{CF} \quad (14)$$

After replacing the dimensionless time, Equation (8), in Equation (14) and solving for F_{cb} will result:

$$F_{cb} = \frac{1052180839(\phi\mu c_t r_w^2)_1}{k_1 t_{\min} \kappa_{CF}} \quad (15)$$

The correction factor for the effect of capacity ratio on the maximum second pressure derivative is:

$$\kappa_{CF} = \left(0.483795 + \frac{0.5162054}{\sqrt{\kappa}}\right)^{-1} \quad (16)$$

And the maximum second pressure derivative is governed by:

$$F_{cb}(t_D)_{\max} = 68633.13/\kappa_{CF} \quad (17)$$

After replacing Equation (8) in the above expression and solving for F_{cb} it yields:

$$F_{cb} = \frac{260269766.27(\phi\mu c_t r_w^2)_1}{k_1 t_{SD\max} \kappa_{CF}} \quad (18)$$

Case 1: $k_1h_1 \leq k_2h_2$

In a similar fashion as for case 1, the resulting equations are:

$$\kappa_{CF} = \left[-0.1291344 + 1.12913435\sqrt{\kappa}\right]^{-1} \quad (19)$$

$$F_{cb}(t_D)_{\min} = 277460.0873/\kappa_{CF} \quad (20)$$

$$F_{cb} = \frac{1052180839(\phi\mu c_t r_w^2)_1}{\kappa_{CF} k_1 t_{\min}} \quad (21)$$

$$\kappa_{CF} = \left[0.2162229 + 0.78377712\sqrt{\kappa}\right]^{-1} \quad (22)$$

$$F_{cb}(t_D)_{\max} = 68633.13/\kappa_{CF} \quad (23)$$

$$F_{cb} = \frac{260269766.27(\phi\mu c_t r_w^2)_1}{k_1 t_{SD\max} \kappa_{CF}} \quad (24)$$

3. EXAMPLES

Although Nooruddin and Rahman (2017) presented two field case examples, they do not provide the complete set of reservoirs, fluids and well data for the estimation of the specific permeability. Therefore, two synthetic examples were provided for demonstration purposes.

3.1 SIMULATED EXAMPLE 1

Figure-7 contains pressure, pressure derivative and second pressure derivative versus time data for a test generated with data from the second column of Table-1. It is required to estimate the specific permeability of the semi-permeable interlayer.

The following information is read from Figure-7.

t_{SDmax} = 3.7 hr t_{min} = 15 hr $(t^*\Delta P')_{r1}$ = 4.06 psi $(t^*\Delta P')_{r2}$ = 3.801 psi

Use Equations (12) and (11) to find the permeability of each layer:

$$k_1 = \frac{70.6(480)(2.2)(1.2)}{100(4.06)} = 220.35 \text{ md}$$

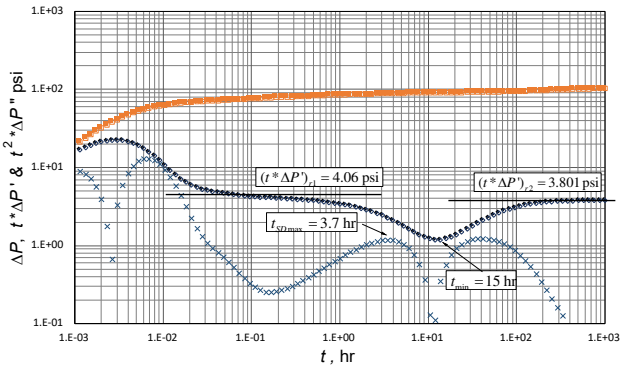

Figure-7. Pressure, pressure derivative and second pressure derivative versus time log-log plot for example 1.

$$k_2 = \left[\frac{4.06}{3.801} - 1\right]\frac{(220.4)(100)}{30} = 50.05 \text{ md}$$

The flow capacity ratio is calculated with Equation (9) to be:

$$\kappa = \frac{k_2}{k_1}\frac{h_2}{h_1} = \frac{50.05}{220.35}\frac{(30)}{(100)} = 0.06814$$

Use Equations (13) and (14) to estimate the flow capacity correction and the specific permeability, respectively, as follows:

$$\kappa_{CF} = \left(0.184439 + \frac{0.81628396}{\sqrt{0.06814}}\right)^{-1} = 0.397519$$

Table-1. Reservoir, fluid and well data for worked examples.

PARAMETER	Example 1	Example 2
k_1, md	220	200
k_2, md	50	500
ϕ_1, %	18	15
ϕ_2, %	18	18
c_{t1}, 1/psi	$1x10^{-6}$	$2x10^{-5}$
c_{t2}, 1/psi	$3x10^{-5}$	$2x10^{-5}$
h_1, ft	100	120
h_2, ft	30	220
r_{w1}, ft	0.3	0.3
r_{w2}, ft	0.3	0.3
s_1	2	0
s_2	2	0
F_C, md-ft	0.0279	0.15
q, bbl/D	480	200
B, rb/STB	1.2	1.25
μ, cp	2.2	3
C, bbl/psi	0.005	0.0005
P_i, psi	1970	5780
k_{v1}, md	6	30
k_{v2}, md	12	10
k_{v1}, md	0.004	0.1
h_0, ft	0.1	0.1
Abs. error 1, %	2.3	-
Abs. error 2, %	0.37	0.815

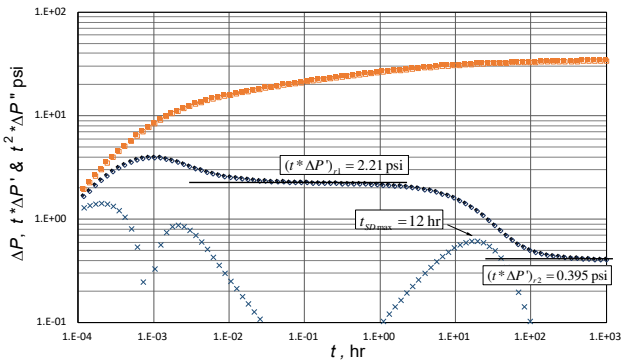

Figure-8. Pressure, pressure derivative and second pressure derivative versus time log-log plot for example 2.

$$F_{cb} = \frac{1052180839(0.18)(2.2)(1\times10^{-5})(0.3^2)}{(220.35)(15)(0.397519)} = 0.02854$$

Use Equations (22) and (24) to find the flow capacity correction and the specific permeability, respectively:

$$\kappa_{CF} = \left(0.483795 + \frac{0.5162054}{\sqrt{0.06814}}\right)^{-1} = 0.406286$$

$$F_{cb} = \frac{260269766.27(0.18)(2.2)(1\times10^{-5})(0.3^2)}{(220.35)(3.7)(0.406286)} = 0.028003$$

3.2. SIMULATED EXAMPLE 2

Figure-8 reports simulated pressure, pressure derivative and second pressure derivative versus time data for a test generated with data from the third column of Table-1. It is required to estimate the specific permeability of the semi-permeable interlayer.

The following information is read from Figure-8.

t_{SDmax} = 12 hr $(t^*\Delta P')_{r1}$ = 2.21 psi $(t^*\Delta P')_{r2}$ = 0.395 psi

Find each layer's permeability with Equations (12) and (11):

$$k_1 = \frac{70.6(200)(3)(1.25)}{120(2.21)} = 199.66 \text{ md}$$

$$k_2 = \left[\frac{2.21}{0.395} - 1\right]\frac{(199.66)(120)}{220} = 500.41 \text{ md}$$

Find the flow capacity ratio from Equation (9);

$$\kappa = \frac{k_2}{k_1}\frac{h_2}{h_1} = \frac{500.41}{199.66}\frac{(220)}{(120)} = 4.594937$$

$$\kappa_{CF} = \left[0.2162229 + 0.78377712\sqrt{4.594937}\right]^{-1} = 0.581862$$

$$F_{cb} = \frac{260269766.27(0.15)(3)(2\times10^{-5})(0.3^2)}{(199.66)(12)(0.581862)} = 0.151222$$

4. COMMENTS ON THE RESULTS

Two synthetic examples were worked to verify the accuracy of the provided equations. One of them devoted to a flow capacity ratio smaller than one and the other for flow capacity ratio higher than one. The methodology uses such characteristic points as the maximum second derivative and the minimum pressure derivative during the effect of the low-permeable interlayer. In all cases the obtained results provided absolute errors lower than 1 %.

Additionally, an excellent equation to estimate the permeability of the adjacent layer was provided and successfully verified. See Equation (11). In the first example the absolute deviation error in the adjacent layer permeability was of 0.1 %. In the second example the error was of 0.08 %.

5. CONCLUSIONS

a) The *TDS* Technique was extended to well pressure test data interpretation of a two-layer system separated by a low-permeable stratum. Equations to estimate the specific permeability using the maximum second pressure derivative and the minimum pressure derivative occurring during the effect of the low-permeable stratum are developed and successfully tested with two synthetic examples with absolute averaged deviation errors lower than 1.2 %.

b) Once the effect of the low-permeable interlayer has vanished, a second plateau develops indicating a domination of radial flow in the adjacent layer. An accurate equation to estimate the permeability of this layer was developed and successfully presented. The deviation error for this equation is lower than 0.1 %.

NOMENCLATURE

B	Oil volume factor, rb/STB
C	Wellborestoragecoefficient, bbl/psi
c_t	Total system compressibility, psi^{-1}
F_{cb}	Specific permeability of the semi-permeable barrier
h	Reservoir thickness, ft
k	Formation permeability, md
P	Pressure, psi
q	Oil flow rate, BPD
r_w	Wellbore radius, ft
s	Skin factor
t	Drawdown time, hr
ΔP	Pressure drop, psi
t_D	Dimensionless time
t_D*P_D'	Dimensionless pressure derivative
$t*\Delta P'$	Pressure derivative, psi
Y	Parameter defined by Equation (A.3)
Z	Parameter defined by Equation (A.4)

Greeks

β	Parameters defined by Equation (A.7) and (A.8)
Δ	Change, drop
ϕ	Porosity, fraction
κ	Flow capacity ratio defined by Equation (9)
κ_{CF}	Flow capacity correction factor
μ	Viscosity, cp
σ	Parameters defined by Equations (A.5) and (A.6)

Suffices

1	Layer 1
2	Layer 2
2*Dmax*	Maximum of second derivative
D	Dimensionless
min	Minimum
r	Radial
w	Well, wellbore
w'	Apparent wellbore

REFERENCES

Al-Wehaibi B. A., Anisur Rahman N. M. and Issaka M. B. 2016, April 25. Estimating the Degree of Inter-Reservoir Communication Between Two Reservoirs Using Advanced Numerical Well Testing Model. Society of Petroleum Engineers. doi:10.2118/182809-MS.

Escobar F.H. 2015. Recent Advances in Practical Applied Well Test Analysis. Nova publishers New York. Published by Nova Science Publishers, Inc. † New York.

Escobar F.H. 2019. Novel, Integrated and Revolutionary Well Test Interpretation Analysis. Intech | Open Mind, England. 278p. DOI: http://dx.doi.org/10.5772/intechopen.81078. ISBN 978-1-78984-850-2 (print). ISBN 978-1-78984-851-9 (online).

Escobar F.H., Jongkittnarukorn K. and Hernandez C.M. 2018. The Power of TDS Technique for Well Test Interpretation: A Short Review. Journal of Petroleum Exploration and Production Technology con ISSN 2190-0566. pp. 1-22. https://doi.org/10.1007/s13202-018-0517-5. 2018.

Escobar F.H., Palomino A.M. and Ghisays-Ruiz A. 2019. An Approximation of Behind Casing Hydraulic Conductivity between Layers from Transient Pressure Analysis. Dyna ISSN 0012-7353, 86(210): 108-114, July - September. DOI: https://doi.org/10.15446/dyna.v86n210.76739.

Escobar F.H., Bonilla L.F. and Hernández C.M. 2018. A practical calculation of the distance to a discontinuity in anisotropic systems from well test interpretation. DYNA, 85(207): 65-73, October - December.

Jalali M., Embry J. M., Sanfilippo F., Santarelli F.J. and Dusseault M.B. 2016, May 25. Cross-flow analysis of injection wells in a multilayered reservoir. Petroleum, 2(3). doi:10.1016/j.petlm.2016.05.005.

Rahman N.M.A. 2014. Measuring behind casing hydraulic conductivity between reservoir layers. US patent and Trademark Office. Patent Application Number 14/182.430. 2014.

Rahman N. M.A, Bin Akresh S. A. and Al-Thawad F. M. 2015. Diagnosis and Characterization of Cross Flow behind Casing from Transient-Pressure Tests. Society of Petroleum Engineers. doi:10.2118/174999-MS. Sep.

Rahman, N. M.A. and Nooruddin, H.A. 2016. Measuring inter-reservoir cross flow rate between adjacent reservoir layers from transient pressure tests. US patent and Trademark Office. Patent Application Number WO/2016/115197.

Nooruddin H. A. and Rahman N. M. A. 2017, March 6. A new analytical procedure to estimate interlayer cross-flow rates in layered-reservoir systems using pressure-transient data. Society of Petroleum Engineers. doi:10.2118/183689-MS.

Tiab D. 1995. Analysis of pressure and pressure derivative without type-curve matching: 1 skin and wellbore storage. J Pet Sci. Eng. 12:171-181.

Appendix A. Expressions complementing Equations (1) and (2) as presented by Rahman and Nooruddin (2016) are:

$$q"(r,t) = \frac{F_{cb}\left[P_2(r,t) - P_1(r,t)\right]}{282.4\pi\mu} \quad \text{(A.1)}$$

$$r_{wa1} = r_{w1}e^{-s_1} \quad \text{(A.2)}$$

$$Y = \frac{k_1\left(F_{cb} + F_2 l\right) + k_2\left(F_{cb} + F_1 l\right)}{k_1 k_2} \quad \text{(A.3)}$$

$$Z = \frac{\left(F_{cb} + F_2 l\right)\left(F_{cb} + F_1 l\right) - F_{cb}^{\ 2}}{k_1 k_2} \quad \text{(A.4)}$$

$$\sigma_1^2 = \frac{Y + \sqrt{Y^2 - 4Z}}{2} \quad \text{(A.5)}$$

$$\sigma_2^2 = \frac{Y - \sqrt{Y^2 - 4Z}}{2} \quad \text{(A.6)}$$

$$\beta_1 = -\frac{F_{cb}}{k_2\sigma_1^2 - F_{cb} - F_2 l} \quad \text{(A.7)}$$

$$\beta_2 = -\frac{F_{cb}}{k_2\sigma_2^2 - F_{cb} - F_2 l} \quad \text{(A.8)}$$

$$q_2\left(t \to \infty\right) B_o = \frac{qB_o k_2}{k_1 + k_2} \quad \text{(A.9)}$$